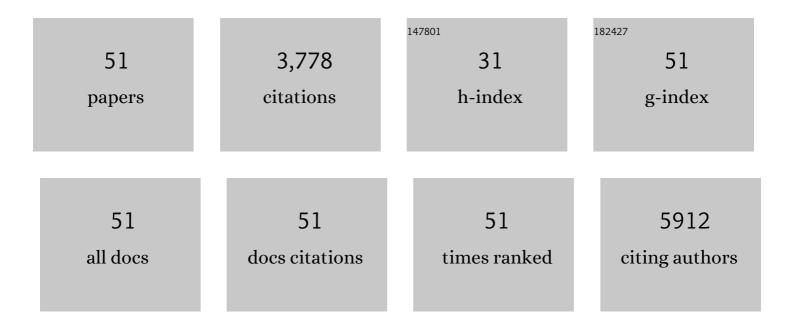


List of Publications by Year in descending order

Source: https://exaly.com/author-pdf/3526798/publications.pdf Version: 2024-02-01



XIN CAL

#	Article	IF	CITATIONS
1	Fiber Supercapacitors Utilizing Pen Ink for Flexible/Wearable Energy Storage. Advanced Materials, 2012, 24, 5713-5718.	21.0	571
2	Integrated power fiber for energy conversion and storage. Energy and Environmental Science, 2013, 6, 805.	30.8	359
3	Nitrogen-doped graphene for dye-sensitized solar cells and the role of nitrogen states in triiodide reduction. Energy and Environmental Science, 2013, 6, 3356.	30.8	265
4	Flexible planar/fiber-architectured supercapacitors for wearable energy storage. Journal of Materials Chemistry C, 2014, 2, 1184-1200.	5.5	207
5	Understanding the solvent-assisted crystallization mechanism inherent in efficient organic–inorganic halide perovskite solar cells. Journal of Materials Chemistry A, 2014, 2, 20454-20461.	10.3	147
6	High-performance perovskite memristor based on methyl ammonium lead halides. Journal of Materials Chemistry C, 2016, 4, 1375-1381.	5.5	118
7	Direct low-temperature synthesis of graphene on various glasses by plasma-enhanced chemical vapor deposition for versatile, cost-effective electrodes. Nano Research, 2015, 8, 3496-3504.	10.4	112
8	<i>In Situ</i> Photodeposited Construction of Pt–CdS/g-C ₃ N ₄ –MnO _{<i>x</i>} Composite Photocatalyst for Efficient Visible-Light-Driven Overall Water Splitting. ACS Applied Materials & Interfaces, 2020, 12, 20579-20588.	8.0	111
9	Flexible fiber-type zinc–carbon battery based on carbon fiber electrodes. Nano Energy, 2013, 2, 1242-1248.	16.0	107
10	Transparent conductive oxide-less, flexible, and highly efficient dye-sensitized solar cells with commercialized carbon fiber as the counter electrode. Journal of Materials Chemistry, 2011, 21, 13776.	6.7	104
11	Conjunction of fiber solar cells with groovy micro-reflectors as highly efficient energy harvesters. Energy and Environmental Science, 2011, 4, 3379.	30.8	101
12	3D Porous Silicon/N-Doped Carbon Composite Derived from Bamboo Charcoal as High-Performance Anode Material for Lithium-Ion Batteries. ACS Sustainable Chemistry and Engineering, 2018, 6, 9930-9939.	6.7	86
13	All-carbon electrode-based fiber-shaped dye-sensitized solar cells. Physical Chemistry Chemical Physics, 2012, 14, 125-130.	2.8	82
14	Strong adsorption of tetracycline hydrochloride on magnetic carbon-coated cobalt oxide nanoparticles. Chemosphere, 2020, 239, 124831.	8.2	82
15	CdS@Ni ₃ S ₂ core–shell nanorod arrays on nickel foam: a multifunctional catalyst for efficient electrochemical catalytic, photoelectrochemical and photocatalytic H ₂ production reaction. Journal of Materials Chemistry A, 2019, 7, 2560-2574.	10.3	71
16	Macro/microfiber-shaped electronic devices. Nano Energy, 2012, 1, 273-281.	16.0	69
17	Application of carbon fibers to flexible, miniaturized wire/fiber-shaped energy conversion and storage devices. Journal of Materials Chemistry A, 2017, 5, 2444-2459.	10.3	67
18	Flexible conductive threads for wearable dye-sensitized solar cells. Journal of Materials Chemistry, 2012, 22, 6549.	6.7	64

Χίν ζαι

#	Article	IF	CITATIONS
19	Facile synthesis of interlocking g-C3N4/CdS photoanode for stable photoelectrochemical hydrogen production. Electrochimica Acta, 2018, 279, 74-83.	5.2	62
20	Flexible, metal-free composite counter electrodes for efficient fiber-shaped dye-sensitized solar cells. Journal of Power Sources, 2012, 215, 164-169.	7.8	61
21	Hierarchical Fe ₂ O ₃ @CNF fabric decorated with MoS ₂ nanosheets as a robust anode for flexible lithium-ion batteries exhibiting ultrahigh areal capacity. Journal of Materials Chemistry A, 2018, 6, 16890-16899.	10.3	61
22	Boosting photocatalytic hydrogen evolution using a noble-metal-free co-catalyst: CuNi@C with oxygen-containing functional groups. Applied Catalysis B: Environmental, 2021, 291, 120139.	20.2	61
23	An amorphous trimetallic (Ni–Co–Fe) hydroxide-sheathed 3D bifunctional electrode for superior oxygen evolution and high-performance cable-type flexible zinc–air batteries. Journal of Materials Chemistry A, 2020, 8, 5601-5611.	10.3	57
24	Simultaneous Encapsulation of Nano-Si in Redox Assembled rGO Film as Binder-Free Anode for Flexible/Bendable Lithium-Ion Batteries. ACS Applied Materials & Interfaces, 2019, 11, 3897-3908.	8.0	53
25	Stretchable, Conductive, and Stable PEDOTâ€Modified Textiles through a Novel In Situ Polymerization Process for Stretchable Supercapacitors. Advanced Materials Technologies, 2016, 1, 1600009.	5.8	48
26	Dye‣ensitized Solar Cells with Vertically Aligned TiO ₂ Nanowire Arrays Grown on Carbon Fibers. ChemSusChem, 2014, 7, 474-482.	6.8	43
27	Hierarchically porous, ultrathin N–doped carbon nanosheets embedded with highly dispersed cobalt nanoparticles as efficient sulfur host for stable lithium–sulfur batteries. Journal of Energy Chemistry, 2020, 50, 106-114.	12.9	43
28	Direct application of commercial fountain pen ink to efficient dye-sensitized solar cells. Journal of Materials Chemistry, 2012, 22, 9639.	6.7	40
29	CdS branched TiO2: Rods-on-rods nanoarrays for efficient photoelectrochemical (PEC) and self-bias photocatalytic (PC) hydrogen production. Journal of Power Sources, 2019, 430, 32-42.	7.8	38
30	Phaseâ€Controllable Growth Ni <i>_x</i> P <i>_y</i> Modified CdS@Ni ₃ S ₂ Electrodes for Efficient Electrocatalytic and Enhanced Photoassisted Electrocatalytic Overall Water Splitting. Small Methods, 2021, 5, e2100878.	8.6	37
31	Synthesis of all-deuterated tris(2-phenylpyridine)iridium for highly stable electrophosphorescence: the "deuterium effect†Journal of Materials Chemistry C, 2013, 1, 4821.	5.5	35
32	Cu Vacancy Induced Product Switching from Formate to CO for CO ₂ Reduction on Copper Sulfide. ACS Catalysis, 2022, 12, 9074-9082.	11.2	35
33	Waveguide fiber dye-sensitized solar cells. Nano Energy, 2014, 10, 117-124.	16.0	32
34	Monodispersed FeCO 3 nanorods anchored on reduced graphene oxide as mesoporous composite anode for high-performance lithium-ion batteries. Journal of Power Sources, 2017, 364, 359-366.	7.8	31
35	Amorphous TiO2 layer on silicon monoxide nanoparticles as stable and scalable core-shell anode materials for high performance lithium ion batteries. Applied Surface Science, 2019, 479, 980-988.	6.1	30
36	Vanadium Nitride Quantum Dots/Holey Graphene Matrix Boosting Adsorption and Conversion Reaction Kinetics for High-Performance Lithium–Sulfur Batteries. ACS Applied Materials & Interfaces, 2021, 13, 30746-30755.	8.0	29

XIN CAI

#	Article	IF	CITATIONS
37	Integration of fiber dye-sensitized solar cells with luminescent solar concentrators for high power output. Journal of Materials Chemistry A, 2014, 2, 926-932.	10.3	27
38	Dual onfined SiO Embedded in TiO ₂ Shell and 3D Carbon Nanofiber Web as Stable Anode Material for Superior Lithium Storage. Advanced Materials Interfaces, 2019, 6, 1801800.	3.7	27
39	Mn doped FeCO3/reduced graphene composite as anode material for high performance lithium-ion batteries. Applied Surface Science, 2018, 428, 73-81.	6.1	26
40	Electrospray synthesis of nano-Si encapsulated in graphite/carbon microplates as robust anodes for high performance lithium-ion batteries. Sustainable Energy and Fuels, 2018, 2, 679-687.	4.9	25
41	Bio-inspired multilayered graphene-directed assembly of monolithic photo-membrane for full-visible light response and efficient charge separation. Applied Catalysis B: Environmental, 2020, 263, 117587.	20.2	24
42	<i>In situ</i> photo-derived MnOOH collaborating with Mn ₂ Co ₂ C@C dual co-catalysts boost photocatalytic overall water splitting. Journal of Materials Chemistry A, 2020, 8, 17120-17127.	10.3	24
43	A CuNi Alloy–Carbon Layer Core–Shell Catalyst for Highly Efficient Conversion of Aqueous Formaldehyde to Hydrogen at Room Temperature. ACS Applied Materials & Interfaces, 2021, 13, 37299-37307.	8.0	24
44	PbCl ₂ -assisted film formation for high-efficiency heterojunction perovskite solar cells. RSC Advances, 2016, 6, 648-655.	3.6	17
45	Carbon oated Cu nanoparticles as a Cocatalyst of g ₃ N ₄ for Enhanced Photocatalytic H ₂ Evolution Activity under Visibleâ€Light Irradiation. Energy Technology, 2019, 7, 1800846.	3.8	17
46	Integrated Bifunctional Oxygen Electrodes for Flexible Zinc–Air Batteries: From Electrode Designing to Wearable Energy Storage. Advanced Materials Technologies, 2022, 7, 2100673.	5.8	12
47	CdS@Mg(OH)2 core/shell composite photocatalyst for efficient visible-light photocatalytic overall water splitting. International Journal of Hydrogen Energy, 2022, 47, 8729-8738.	7.1	11
48	Ni Foam Supported TiO ₂ Nanorod Arrays with CdS Branches: Type II and Z‧cheme Mechanisms Coexisted Monolithic Catalyst Film for Improved Photocatalytic H ₂ Production. Solar Rrl, 2022, 6, .	5.8	9
49	Enhanced photocatalytic oxidation and biodegradation of polyethylene films with PMMA grafted TiO ₂ as proâ€oxidant additives for plastic mulch application. Polymer Composites, 2018, 39, 3409-3417.	4.6	7
50	Zinc-assisted mechanochemical coating of a reduced graphene oxide thin layer on silicon microparticles to achieve efficient lithium-ion battery anodes. Sustainable Energy and Fuels, 2019, 3, 1258-1268.	4.9	5
51	Low-cost nanocarbon electrodes on arbitrary fibrous substrates as efficient bifacial photovoltaic wires. RSC Advances, 2017, 7, 9653-9661.	3.6	4